Inelastic neutron scattering from liquid and solid hydrogen at high momentum transfer

W. Langel*
Institut Max von Laue-Paul Langevin, 156 X Centre de Tri, F-38042 Grenoble, France

D. L. Price
Materials Science Division, Argonne National Laboratory, Argonne, Illinois 60439

R. O. Simmons
Department of Physics, University of Illinois at Urbana-Champaign, Urbana, Illinois 61801

P. E. Sokol
Lyman Laboratory of Physics, Harvard University, Cambridge, Massachusetts 02138
(Received 2 March 1987; revised manuscript received 2 May 1988)

Solid and liquid para-hydrogen and a solid mixture of ortho- and para-hydrogen have been studied by inelastic neutron scattering at momentum transfers from 5 to 30 Å^{-1}. The observed scattering function can be interpreted in terms of scattering from independent hydrogen molecules using the impulse approximation when internal excitations of the molecules are included. Scattering peaks are observed at the recoil energy, shifted by the energy of the internal rotational transitions, and broadened by the translational motion of the molecules. The peaks can be fitted by Gaussian functions, showing that, to within the accuracy of the measurement, the translational momentum distribution of the hydrogen molecules in the condensed phases has a Gaussian form. The kinetic energy of the para-hydrogen molecules at 1 bar is 76±9 K in the solid at 10 K and 63±6 K in the liquid at 17 K. The kinetic energy for the ortho component in the solid ortho-para mixture is estimated to be the same as for the para solid within the experimental error, although extraction of quantitative information is more difficult because of the complicated spectra.

I. INTRODUCTION

Hydrogen is the lightest molecule which forms condensed phases. The light mass of the molecule and the weak intermolecular forces lead to pronounced quantum effects in the solid and liquid, the most prominent being the high contribution of the kinetic energy of the zero-point motion to the total energy of the system at low temperatures. For example, the melting point[1] of the H_2 crystal is only about one-tenth of its Debye temperature of 120 K, as compared to more classical solids where the melting point is usually larger than the Debye temperature.

Molecular hydrogen has been the subject of several neutron scattering studies due to its interesting properties in the condensed phases and its high neutron cross section. Most experiments have been carried out at relatively low energy and momentum transfers. In the solid, the phonon dispersion relation and the Debye-Waller factor have been measured using coherent scattering,[2] and the phonon density of states has been measured using incoherent scattering.[3] In the liquid, a collective excitation was found which corresponds to the phonons in the solid.[4]

Neutron scattering measurements at high momentum transfers will be dominated by scattering from single particles. At sufficiently high momentum transfer Q, the impulse approximation (IA) is valid and neutron scattering measurements can be used to directly determine the single-particle momentum distribution $n(p)$. The momentum distribution is of particular interest since the average kinetic energy per atom may then be directly determined and compared with the results of microscopic theories of the condensed phase. Similar measurements on helium, the most extensively studied quantum system,[5] have shown that the IA provides an excellent description of the observed scatteirng for Q's above 10 Å^{-1}. The experimentally determined $n(p)$ has been compared with the results of microscopic calculations[6] using both variational and Monte Carlo techniques, and the agreement is, on the whole, quite good.

In the present paper we report measurements of the scattering function $S(Q,E)$ of a condensed molecular system (hydrogen) at high momentum transfers. Our results are interpreted using the impulse approximation and a model where the internal excitations of the molecule (rotations and vibrations) are decoupled from the translational degrees of freedom. We find that this model provides a good description of the observed scattering and allows us to extract the kinetic energy in the liquid and solid phases.

Microscopic theoretical studies of the condensed phases in hydrogen are not as extensive as in helium. No published theoretical calculations of the kinetic energy are known to us. Therefore, current estimates of the kinetic energy are based primarily on the Debye model[7] which may not provide a good representation of quantum solids, where the zero-point motion plays an important

role. The measurements presented here provide a direct measure of the kinetic energy, without reference to any particular model, that may be compared with theoretical calculations of the condensed phases of hydrogen.

II. THEORETICAL BACKGROUND

A. Deep inelastic neutron scattering

In the limit of large momentum transfer Q, the scattering function may be expressed in terms of the scattering of individual particles from a bound initial state, determined by the many-body interactions in the sample, to a free particle final state. This is the well-known impulse approximation,[8] which leads to a general form for the scattering cross section for a monatomic system of the form

$$\frac{d^2\sigma}{d\Omega dE}=\frac{k_f}{k_i}b^2S(Q,E)\ ,$$
$$S(Q,E)=\int n(|\mathbf{p}|)\delta\left[E-E_r-\frac{\hbar\mathbf{Q}\cdot\mathbf{p}}{M}\right]d\mathbf{p} \tag{2.1}$$

where b is the bound-atom scattering length, k_i and k_f are the initial and final neutron wave vectors, $n(|\mathbf{p}|)$ is the distribution of atomic momenta, $\mathbf{p}$, and $E_r=\hbar^2Q^2/2M$ is the recoil energy corresponding to the atomic mass M of the scattering atoms. The approximation is generally considered to be valid when $E_r\gg\hbar\omega_c$, where ω_c is a characteristic phonon frequency. This corresponds to a physical picture in which the surrounding atoms do not move appreciably during the time in which the neutron interacts with the scattering nuclei.

For a harmonic crystal the impulse approximation may be derived from a multiphonon expansion of the scattering starting from the low Q limit. Multiphonon transitions become more prominent and gain intensity as Q increases.[9] At sufficiently high Q, the envelope of the multiphonon scattering approaches the form given by the impulse approximation. The condition for this is readily seen to be a small Debye-Waller factor $[\exp(-Q^2\langle u^2\rangle/3)\ll 1]$ which for a set of harmonic oscillators reduces to the condition $E_r\gg\hbar\omega_c$, as before.

The Gaussian form for the momentum distribution

$$n(p)=\frac{1}{(2\pi\sigma_p^2)^{1/2}}\exp\left[\frac{-p^2}{2\sigma_p^2}\right] \tag{2.2}$$

holds a special significance. It is the expected form for classical systems obeying Maxwell-Boltzmann statistics and, using the central limit theorem, when many interacting normal modes are present.[10] This form has been observed in many systems, including quantum liquids and solids such as the solid and normal liquid phases of helium. The scattering, in the impulse approximation, then has the simple form

$$S(Q,E)=\frac{1}{(2\pi\sigma_s^2)^{1/2}}\exp\left[-\frac{(E-E_r)^2}{2\sigma_s^2}\right]\ , \tag{2.3}$$

which is a Gaussian with a standard deviation $\sigma_s=\hbar Q\sigma_p/M$ centered at the recoil energy.

The kinetic energy per atom may be evaluated directly from the momentum distribution

$$\langle E_k\rangle=\int\frac{\mathbf{p}\cdot\mathbf{p}}{2M}n(\mathbf{p})d\mathbf{p} \tag{2.4}$$

which gives, in terms of the measured width of the observed scattering

$$\langle E_k\rangle=\frac{3M\sigma_s}{2\hbar^2Q^2} \tag{2.5}$$

where σ_s is the observed standard deviation of the scattering, Q is the momentum transfer, and $\langle E_k\rangle$ is the kinetic energy. In an ideal gas the kinetic energy is simply $\frac{3}{2}T$, where T is the temperature of the gas. In solids, $\langle E_k\rangle$ is $\frac{3}{4}\Theta_E$ in the Einstein model and $\frac{9}{16}\Theta_D$ in the Debye model.

B. Scattering from molecules

In the case of molecules with internal degrees of freedom, Eq. (2.1) can readily be generalized if the internal excitations are decoupled from the translational degrees of freedom. Then, Eq. (2.1) becomes

$$\frac{d^2\sigma}{d\Omega dE}=\frac{k_f}{k_i}\sum_n b_n^2S_n(Q,E)\ ,$$
$$S_n(Q,E)=f_n\int n(|\mathbf{p}|)\delta\left[E-E_r-E_n-\frac{\hbar\mathbf{Q}\cdot\mathbf{p}}{M}\right]d\mathbf{p}\ . \tag{2.6}$$

The summation is over all internal excitations of the target molecule and b_n, f_n, and E_n represent the scattering length, structure factor, and excitation energy of the nth internal level. For a Gaussian distribution of translational momenta, this reduces to a series of Gaussian functions of different weights centered at (E_n+E_r) and having a standard deviation determined by the translational momentum distribution only.

The classical treatment of the scattering from molecules which are rotationally excited in the scattering process gives the recoil mass in terms of the Sachs-Teller mass tensor.[11] This should also represent the limit of the quantum-mechanical expression when the energy spacing of the internal levels is compared with the peak width (or, equivalently, with the energy resolution of the measurement). If, on the other hand, the transitions between the internal levels can be resolved, Eq. (2.6) with the molecular mass M should be used in the form given, and each internal transition is broadened by the translational momentum distribution. The structure factor governing the integrated intensity of the line corresponding to this transition should be calculated on the basis of the internal degrees of freedom only, as pointed out by Griffin and Jobic.[12]

C. Molecular hydrogen

The scattering function of hydrogen has been calculated by Sarma[13] and by Young and Koppel.[14] Both papers take rotations into account and assume a complete separation of translational and internal modes; in addition, the Young and Koppel calculation includes the stretch

vibrations of the H_2 molecule which are assumed to be decoupled from the rotational motion. The energies of the rotational levels, characterized by the quantum number J, are given by $E_{\rm rot}=J(J+1)B$, where $B=7.35$ meV. The vibrational energy levels, characterized by quantum number ν, are given by $E_{\rm vib}=(\nu+\frac{1}{2})\hbar\omega_{\rm vib}$, where $\hbar\omega_{\rm vib}=516$ meV. With the incident energies used in the present experiments, it is clearly important to allow for both kinds of internal transition.

The central feature in both calculations is the decoupling of the translational motion from the internal excitations of the molecule. Thus, these models should also be valid in the solid where spectroscopic studies have shown that the hydrogen molecules behave as nearly free rotors.[15] The primary modification to the calculations is the replacement of the ideal-gas momentum distribution, a Maxwellian with a width determined by the temperature, by the more general form of Eq. (2.2) to take into account the larger zero-point motion in the condensed phases. With this replacement the formalism of Young and Koppel provides an excellent framework for analyzing the present data. In particular, explicit expressions for the appropriate molecular scattering lengths and structure factors appearing in Eq. (2.6) are given.

An important result of the Young and Koppel calculation is that the scattering cross section depends on the parity of the initial and final internal states of the hydrogen molecule. At the temperature of these experiments, the molecules are predominantly in their vibrational and rotational ground states, the latter being $J=0$ for para-H_2 and $J=1$ for ortho-H_2. In the case of para-H_2, the scattering to even-J states is then proportional to the coherent cross section σ_c, while that to odd-J states is proportional to the incoherent cross section σ_i. Since $\sigma_i \gg \sigma_c$ for natural hydrogen (the bound-atom values are $79.9b$ and $1.8b$, respectively[16]), this means that in para-H_2 only scattering to odd-J states should be observed. The form for the structure factor[14] of Eq. (2.6) when the initial state is pure para-H_2 then becomes

$$f_{J\nu}=\frac{1}{\nu!}\left[\frac{Q^2}{4M\omega_{\rm vib}}\right]^2(2J+1)C^2(0,J,J;00)\times\left|\int_{-1}^{+1}d\mu\mu^{\nu}\exp\left[-\frac{\hbar Q^2\mu^2}{8M\omega_r}+i\frac{Qa\mu}{2}\right]P_J(\mu)\right|^2, \tag{2.7}$$

where J and ν are the quantum numbers of the final rotational and vibrational states respectively, C is a Clebsch-Gordan coefficient, a is the distance between the two protons in the molecule, and P_J is a Legendre polynomial of order J. If the final state does not involve excition of the vibrational levels, Eq. (2.7) simplifies to

$$f_J=(2J+1)C^2(0,J,J;00)\,|\,2i^J j_J(Qa/2)\,|^2, \tag{2.8}$$

where j_J is the spherical Bessel function of order J. This simple form arises from the model since the rotational states are assumed to be those of a simple ideal rigid rotor (i.e., the rotational wave functions are proportional to the spherical harmonics).

For ortho-H_2 the situation is more complex. The cross section for transitions where the change in J is odd is σ_i and the cross section for transitions where the change in J is even is $3\sigma_c+2\sigma_i$. Thus, in ortho-H_2 scattering to all final state should be observed as long as the energy conservation condition can be met and the structure factor is large enough at the momentum transfer of the measurement. This leads to a considerably more complex spectrum.

The simple model of an ideal rotational and vibration spectrum that do not interact is not entirely appropriate for hydrogen. Raman scattering measurements for H_2 vapor indicate that the vibrations and rotations are not completely decoupled.[17] As a consequence, the expression for the rotational energy levels takes the modified form

$$E_{\rm rot}=J(J+1)B_\nu-[J(J+1)]^2D_\nu+[J(J+1)]^3H_\nu-\cdots, \tag{2.9}$$

where ν signifies the associated vibrational state. The first few terms of this expansion for $\nu=0$ are $B_0=7.356$ meV, $D_0=5.689\times10^{-3}$ meV, and $H_0=6.446\times10^{-6}$ meV. For small values of J the energy levels are essentially given by the free rotor expressions. For higher J values small deviations from the ideal rigid rotor appear. To a first approximation, we may simply replace the ideal rigid rotor values for the excitation energies in Eq. (2.6) with the more accurate values in Eq. (2.9).

III. EXPERIMENTAL PROCEDURE

The measurements were carried out using the Low-Resolution Medium Energy Chopper Spectrometer (LRMECS) at the Intense Pulsed Neutron Source (IPNS) at Argonne National Laboratory.[18] LRMECS is a time-of-flight (TOF) spectrometer with a chopper before the sample to monochromate the pulsed white beam from the spallation source. Incident energies of 500 and 1900 meV were used in these measurements. The Fermi chopper had a pulse width and slit curvature that were optimized for 500-meV neutrons. Operation at 1900 meV resulted in some degradation of both resolution and intensity. Detectors are located at scattering angles between 2.6° and 116°; in this measurement useful data were obtained between 15° and 75°. This represents Q's between 5 and 16 Å^{-1} at 500 meV incident energy and Q's between 9 and 31 Å^{-1} at 1900 meV incident energy.

The samples were condensed into a slab-shaped cell which consisted of 20 aluminum capillaries, each with an internal diameter of 1.3 mm. This design reduced the contamination of the observed spectra by multiple scattering within the sample. The cell, which was attached to a Displex closed-cycle refrigerator, was mounted on a vertical plane at 45° to the incident beam (transmission geometry) and extended over the full beam area of 5 cm wide by 10 cm high. The temperature was measured with thermocouples at the top and bottom of the cell; the steady-state difference between the top and bottom was about 1 K.

Two different samples were studied under various conditions. Nearly pure para-hydrogen was obtained by

holding liquid in the cell in contact with a ferromagnetic catalyst,[1] which enhances the ortho-para conversion, for two days prior to the experiment. The catalyst was located in a portion of the cell not exposed to the neutron beam to avoid contamination of the scattering. Measurements of this sample were carried out at 10 K in the solid and 17 K in the liquid. After removing the catalyst, a second sample of normal H_2, expected to have an initial concentration of 75%, was studied at 10 K immediately after condensation of the sample. Due to conversion in the solid during the course of the measurement the mean ortho concentration of this sample was approximately 40%, as discussed in Sec. IV.

The data were analyzed using standard programs[19] developed to handle time-of-flight data from the chopper spectrometers at IPNS. The analysis included correction for detector efficiency obtained from measurements on a vanadium reference sample, subtraction of the empty cell scattering, conversion from time-of-flight to energy scales, and interpolation of the spectra taken at constant detector angle to constant momentum transfer. The results presented here have all been converted to constant Q to facilitate comparison with the theoretical expressions for the intensity of the transitions.

To accurately determine the true scattering function, the effects of instrumental resolution and multiple scattering must be taken into account. Time-of-flight instruments at spallation sources have a complicated asymmetric resolution function due to the asymmetric shape of the pulse of neutrons from the moderator, the transmission through the chopper, and the finite rotational speed of the chopper. In general, the resolution is a complex function that is not amenable to simple solution.[20] However, an analytic calculation[21] of the resolution is possible if all the source terms are represented as Gaussians of the appropriate width. This approximation, which we use here, results in a Gaussian resolution function which greatly simplifies the analysis of the results.

Multiple scattering can provide a substantial contribution to the observed scattering, particularly in strongly scattering samples such as hydrogen. To minimize the contribution of multiply scattered neutrons we used the sample cell described above. The multiple scattering is determined primarily by the dimension of the sample in the direction of the incident beam, since the cross section is largest for coherent scattering which occurs at small energy and momentum transfer, and is minimized by using a sample with small dimensions in the direction of the beam, as has been done here. The contribution of multiple scattering to the total scattering was estimated using a Monte Carlo simulation[22] of the scattering. We find, for our sample geometry, that the multiple scattering appears as small, nearly constant background that does not appreciably distort the shape of the observed peaks.

IV. RESULTS

Figure 1 shows examples of constant-Q spectra taken with an incident energy of 500 meV. All spectra consist of one or more peaks which are considerably broader than the instrument resolution. The positions, widths,

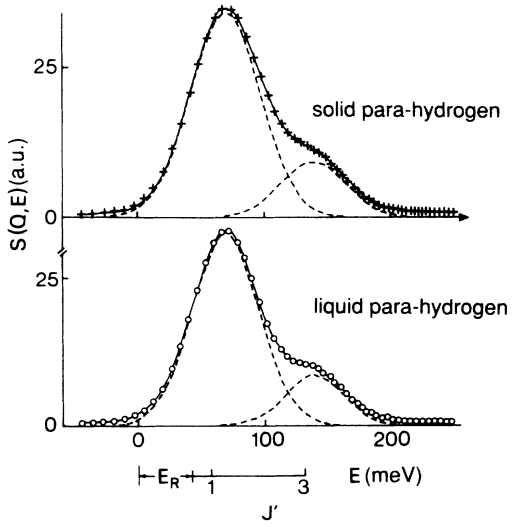

FIG. 1. Spectra of liquid and solid para-hydrogen at a momentum transfer of $Q=7$ Å^{-1}. The incident energy was 500 meV. The recoil-shifted transitions from the $J=0$ ground state to final states $J'=1$ and 3 are seen. The solid line is a fit by the sum of two Gaussians (dashed lines) and a straight line background.

TABLE I. Amplitudes (A), energies (E) and standard deviations (σ_0) of the fitted peaks for solid hydrogen spectra at 10 K and an incident energy $E_0=500$ meV. Standard deviations in parentheses have large associated errors and were not used in calculation of kinetic energy. The intrinsic standard deviation (σ_e) is obtained by correcting for the resolution (σ_r) using $\sigma_e=(\sigma_0^2-\sigma_r^2)^{1/2}$. The momentum transfer is in Å^{-1}, the amplitude in arbitrary units, and the standard deviations in meV.

Q	J'	A	E	σ_0	σ_r	σ_e
5.0	1	45.2	44.0	24.2	19.0	15.0
	3	2.4	115.5	(18.9)		
6.0	1	42.2	55.0	25.8	18.5	18.5
	3	5.1	124.9	22.2	14.5	16.8
7.0	1	34.0	68.9	27.3	17.9	20.6
	3	9.0	138.0	25.4	13.9	21.3
8.0	1	21.4	83.7	28.4	17.3	22.5
	3	14.1	152.8	28.5	13.3	25.2
9.0	1	11.6	97.2	28.5	16.6	23.2
	3	18.0	168.7	31.0	12.7	28.3
10.0	1	4.3	111.0	(26.5)		
	3	21.3	188.1	33.2	12.0	31.0
	5	1.3	307.4	(32.5)		
11.0	3	21.1	211.2	35.1	11.3	33.2
	5	2.0	328.4	(26.8)		
12.0	3	20.5	234.6	38.1	10.6	36.6
	5	5.9	361.3	(45.3)		
13.0	3	17.7	259.0	40.6	9.8	39.4
	5	7.8	382.4	41.9	4.0	41.7
14.0	3	13.1	284.0	46.3	9.0	45.4
	5	10.	418.4	(46.2)		
15.0	3	8.9	314.0	(63.7)		
	5	11.8	446.0	(38.3)		
16.0	3	5.4	343.6	(77.4)		
17.0	3	3.1	358.7	(83.5)		

and relative intensities of these peaks depend very sensitively on the momentum transfer. Spectra of liquid and solid para-H_2, however, corresponding to the same momentum transfer, are very similar to each other. Only the linewidths are different, being wider for the solid than for the liquid.

The peaks in the spectra from para-H_2 samples taken with an incident energy of 500 meV are reasonably well separated. These peaks should occur at the recoil energy, shifted by the energy of the rotational transitions. In order to assign them, the position, width, and amplitude of each peak were found by a chi-square fit to a model scattering function consisting of a sum of Gaussians plus a small constant background. The results of these fits for the spectra taken with an incident energy of 500 meV are presented in Table I for the solid and in Table II for the liquid.

The position of the peaks versus the square of the momentum transfer is shown in Fig. 2. As predicted by the theory, the peak positions fall on straight lines with intercepts equal to the transition energy from the rotational ground state $J=0$ to the final state $J'=1,3,5,\ldots$ and a slope which corresponds to the recoil energy of a free hydrogen molecule. The rotational transition energies have been calculated using Eq. (2.9), which gives somewhat better agreement for the higher rotational transitions than the rigid rotor values used in the original calculation of Young and Koppel.

Each transition to a given state is found only in a limited Q range. This point is illustrated in Fig. 3, which shows the peak intensity as a function of Q for each J' transition and the predictions of the Young and Koppel calculations for the scattering strength. It is clear that for each J' there is a value of Q where the intensity is highest, and for Q values greater or (if $J'>1$) less than this, the intensity falls off and the transition is unobservable. Overall, the Young and Koppel model predicts the qualitative behavior of the scattering intensity quite well.

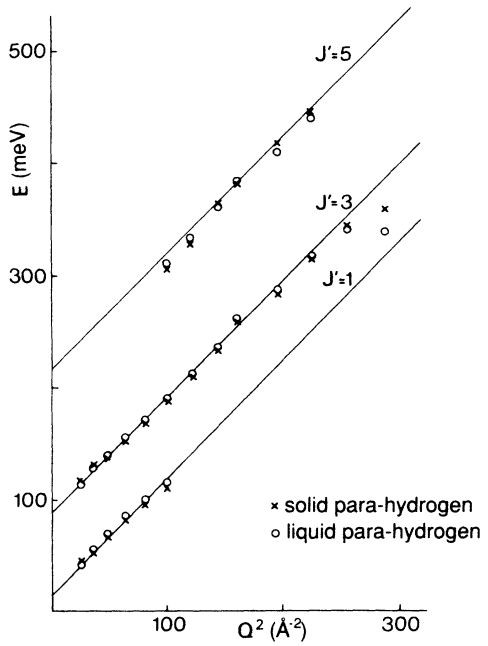

FIG. 2. Plot of peak energy vs Q^2 in the spectra of liquid and solid para-H_2 for an incident energy of 50 meV. The statistical errors (standard deviations) of the fitted values are within the size of the points. The straight lines have a slope corresponding to $M=2$ amu and an intercept equal to the energy of the transition from the ground state ($J=0$) to the final states $J'=1$, 3, and 5, calculated using Eq. (2.9).

TABLE II. Amplitudes, energies and standard deviations of fitted peaks for the liquid-hydrogen spectra at 17 K and an incident energy of $E_0=500$ meV. Notations are the same as in Table I.

Q	J'	A	E	σ_0	σ_r	σ_e
5.0	1	42.5	44.2	23.6	19.0	13.9
	3	2.2	117.0	(16.7)		
6.0	1	40.0	55.6	24.8	18.5	16.6
	3	4.6	126.7	20.4	14.5	14.3
7.0	1	32.5	69.6	26.1	17.9	19.0
	3	8.4	140.1	22.9	13.9	18.2
8.0	1	21.0	85.9	27.7	17.3	21.7
	3	13.2	155.9	25.2	13.3	21.4
9.0	1	11.8	101.1	28.7	16.6	23.4
	3	16.8	171.6	27.5	12.7	24.4
10.0	1	4.6	116.1	(26.3)		
	3	20.5	189.9	30.4	12.0	27.9
	5	1.4	311.1	(28.1)		
11.0	3	20.9	212.2	32.7	11.3	30.7
	5	2.5	334.3	(31.7)		
12.0	3	19.7	236.3	34.8	10.6	33.1
	5	5.0	361.8	(38.4)		
13.0	3	17.3	260.7	38.0	9.8	36.7
	5	7.3	383.7	36.6	4.0	36.4
14.0	3	12.5	287.7	42.7	9.0	41.8
	5	8.3	409.8	(34.3)		
15.0	3	8.4	315.5	(57.5)		
	5	8.7	440.4	(32.3)		
16.0	3	5.0	341.6	(72.9)		
17.0	3	2.6	337.8	(62.9)		

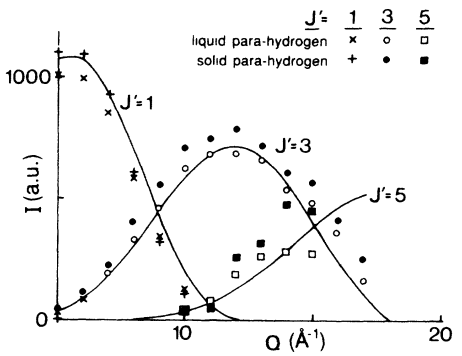

FIG. 3. Plot of the relative intensities (amplitude times standard deviation) of the rotational transitions vs Q for liquid and solid para-hydrogen, compared with the theoretical values (solid lines) from Young and Koppel (Ref. 14). The statistical errors (standard deviations) in the fitted values are within the size of the points.

It correctly predicts the fall-off of the $J=0$ to $J'=1$ transition as Q increases and the subsequent buildup and decay of the $J'=3$ and $J'=5$ transitions. However, quantitative differences exist between the experimental results and the theoretical predictions; these will be discussed later.

Intrinsic peak widths due to the translational momentum distribution were extracted from the fitted Gaussians by correcting for the spectrometer resolution. Using the Gaussian approximation for the instrumental resolution, the resolution simply adds in quadrature to the intrinsic peak width.[23] Since the rotational and translational motion are decoupled, we expect the intrinsic widths to be the same for different rotational lines observed at a given Q. The width obtained from the fits, corrected for instrumental resolution, are shown in Fig. 4. The expected behavior in the IA (linear dependence of σ on Q) is clearly reproduced in the resolution-corrected data. Apart from some data points representing peaks with small amplitudes or peaks which are only partly covered by the available energy-transfer range, both cases resulting in a large uncertainty in the peak width, we find good agreement with the behavior predicted by the IA. From the slope of the straight lines fitted to the data in Fig. 4, we find mean kinetic energies of $\langle E_k \rangle = 76 \pm 9$ K in the solid phase (10 K) and $\langle E_k \rangle = 63 \pm 6$ K in the liquid phase (17 K).

The difference in the kinetic energy between the solid and the liquid measurements is within the respective errors for the kinetic energies. However, these errors are determined by considering the overall best fit of the width measurements to the IA prediction. These fits include

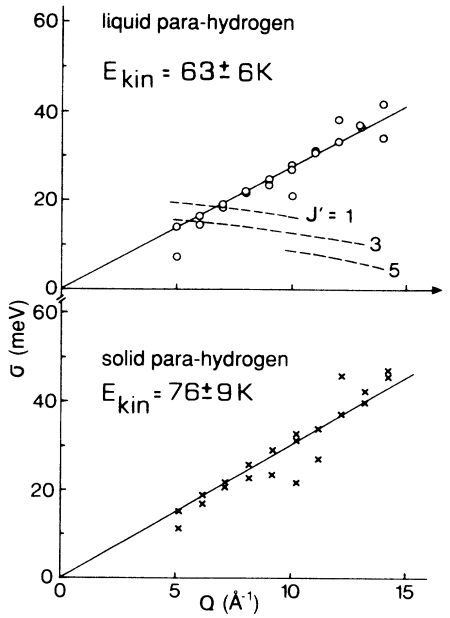

FIG. 4. Plot of the intrinsic width of the individual rotational transitions vs momentum transfer Q for liquid and solid para-H_2. The statistical errors (standard deviations) in the values are within the size of the points. The dashed lines in the upper figure show the instrumental resolution in terms of the equivalent Gaussian width.

several sources of error not directly related to the relative width of the observed spectra. A more sensitive test[24] is to compare the fitted widths in the solid and the liquid at each Q. This comparison is shown in Table III. The average value of the ratio of the width in the solid to the width in the liquid is 1.106 ± 0.0425, indicating that the kinetic energy in the solid is a factor of 1.22 ± 0.09 greater than the kinetic energy in the liquid. This most likely represents the increased freedom of the molecules in the liquid phase.

The value of $\langle E_k \rangle$ obtained for the para-H_2 solid may be compared with the Debye temperature. The Debye temperature may be determined using several methods.[25] Heat-capacity measurements give $\Theta_D = 125$ K at $T=0$ and 99 K at the triple point, a strong variation with temperature. The Debye temperature may also be determined from density and sound velocity measurements. Using these data, Θ_D is 108 K at $T=0$ and 104 K at the triple point, showing a much smaller variation with temperature than the values obtained from heat-capacity data. Θ_D may also be extracted from infrared measurements, giving values in agreement with the density and sound velocity values. Near the triple point all methods give comparable values for Θ_D and would give a kinetic energy at 1 K of 60–65 K, significantly lower than our measured value in the solid.

Microscopic calculations, which explicitly take into account correlations between molecules and the hard-core repulsion, give somewhat better agreement with the measured values. A recent first-principles calculation by Goldman[26] gives $\langle E_k \rangle = 68$ K for the solid at 10 K, agreeing with the experimental value within the estimated error.

The Debye model does not formally describe the liquid state. However, Debye temperatures for the liquid have been determined from heat-capacity measurements.[25] These range from 106 K at the triple point to 92 K at 20 K. Thus, using the same arguments as in the solid, we

TABLE III. Comparison of the peak widths in the solid at 10 K and in the liquid at 17 K.

Q	σ_s	σ_l	$R=\sigma_s/\sigma_l$
5.0	15.0	13.9	1.079
6.0	18.5	16.6	1.114
	16.8	14.3	1.175
7.0	20.6	19.0	1.084
	21.3	18.2	1.170
8.0	22.5	21.7	1.037
	25.2	21.4	1.177
9.0	23.2	23.4	.991
	28.3	24.4	1.160
10.0	31.0	27.9	1.111
11.0	33.2	30.7	1.081
12.0	36.6	33.1	1.106
13.0	39.4	36.7	1.074
	41.7	36.4	1.146
14.0	45.4	41.8	1.086
$\bar{R}$			1.106±.0425

expect the kinetic energy to be on the order of 56 K, which is again lower than our observed value but by less than in the solid.

The much lower kinetic energy in the liquid is somewhat surprising. The Debye model predicts a slightly lower $\langle E_k \rangle$ for the liquid, due to the lower density of the liquid.[25] The density in the liquid at 1 bar and 17 K is 27.5 cm^3 cm/mole while in the solid at 10 K it is 23.31 cm^3/mole. This 15% change in the density is consistent with the slightly lower $\langle E_k \rangle$ in the liquid predicted by the Debye model.

The higher-kinetic energy in the solid phase most likely results from correlations between the molecules that are not included in the simple Debye model. Correlations between molecules can increase the kinetic energy if they force the atomic wave functions to overlap the hard-core region of the potential. Thus, Goldman's calculation, which includes correlations between the molecules, predicts a larger kinetic energy than the Debye model, which essentially ignores correlations.

It is possible to fit all peaks in the spectra simultaneously using the structure factors from Young and Koppel. However, the resultant fits are not satisfactory as those obtained using multiple independent Gaussians. It is clear from Fig. 3 that, while the Q dependence of the intensities is qualitatively reproduced by the Young and Koppel formalism, real discrepancies remain. For example, the measured intensities appear to be above the Young and Koppel prediction for $J'=3$ but below them for $J'=1$.

The reasons for the deviations of the experimental intensities from the calculated structure factors are not clear. The vibrational-rotational coupling, neglected in the Young and Koppel calculation, may affect the intensities as well as the energies of the rotational transitions. It is also possible that the rotations are not in fact completely free in the condensed phases, in which case the rotational wave functions and hence the matrix elements of the transitions would be perturbed.

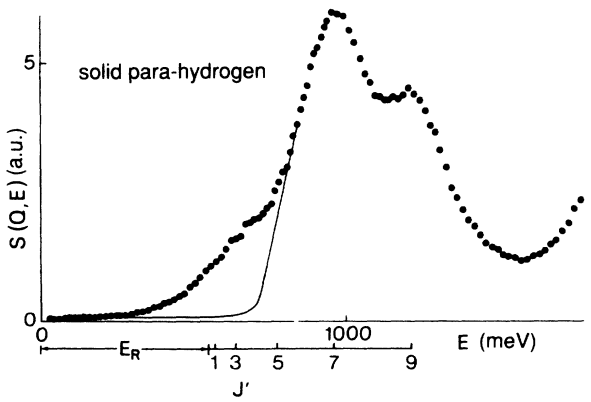

FIG. 5. Spectra of solid para-hydrogen at a momentum transfer of 23 $Å^{-1}$, taken with an incident energy of 1900 meV. The transitions to $J'=7$ and 9 are well resolved. The solid line is a guide-to-the-eye extrapolation of the $J'=7$ transition. The transitions to $J'=1$, 3, and 5 form the wing on the low-energy-transfer side of the peak.

The scattering function of solid para-H_2 was also measured with an incident energy of 1900 meV as shown in Fig. 5. Since the resolution width of the instrument at this energy is much greater than at 500 meV, the lower rotational lines are no longer resolved in these spectra. The width of the observed lines at this incident energy is determined primarily by the instrumental resolution. As the plot of energy versus Q^2 (Fig. 6) shows, transitions to the $J'=7$, 9, and 11 rotational levels are seen in addition to those observed at the lower neutron energies (the energy values represent estimates since a Gaussian fit was not performed). Most of the observed peaks can be assigned to rotational transitions. However, there is some evidence at lower Q values of the stretch vibration at 516 meV, although the structure factor is small due to the small amplitudes of motion encountered at this energy and temperature. At larger Q values, the conditions of the measurements reported here largely correspond to scattering from rigid molecules.

In these measurements the effective mass entering the recoil energy E_r in Eq. (2.6) is the mass of the hydrogen molecule, i.e., $M=2$ amu. The classical picture which describes the rotational excitations on the basis of the Sachs-Teller mass tensor suggests an effective mass of $M=\frac{4}{3}$ amu for the hydrogen molecule. This should ap-

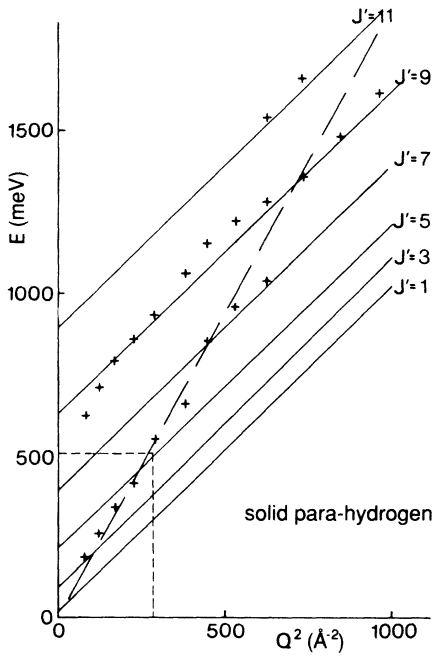

FIG. 6. Plot of the estimated peak energy vs Q^2 for the spectra recorded with an incident energy of 1900 meV. The dashed line through the origin corresponds to an effective mass of $\frac{4}{3}$, as predicted by the Sachs-Teller mass tensor. The straight lines have a slope corresponding to $M=2$ amu and an intercept equal to the energy of the transition from the ground state ($J=0$) to the final states $J'=1$, 3, 5, 7, 9, and 11 calculated using Eq. (2.9). The rectangle marked off by dotted lines represents the region covered by Fig. 2, in which the different rotational levels are resolved.

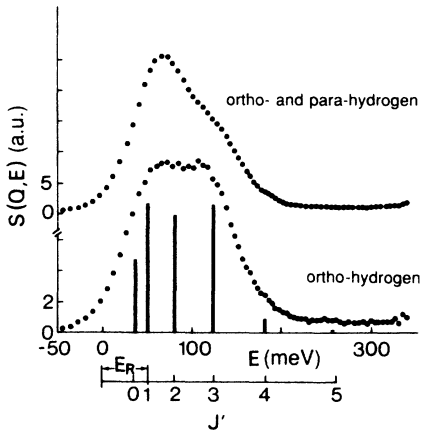

FIG. 7. Spectra of a solid ortho-para mixture at $Q=7$ Å^{-1}. The upper trace shows the observed spectrum. The lower trace shows the difference between the mixture spectrum and the para spectrum multiplied by 0.4 The vertical lines indicate calculated positions and relative intensities of the recoil-shifted rotational transitions.

ply in the situation where the different rotational lines cannot be resolved. In Fig. 6 a line with zero intercept and slope corresponding to $M=\frac{4}{3}$ amu is plotted. It does appear to pass through the energy regions where the strongest scattering occurs at a given momentum transfer. It is clear that very much higher momenta, such that $E_r \gg E_{\rm vib}$, would be required to observe recoil scattering corresponding to free hydrogen atoms, $M=1$ amu.

We have also measured the spectra of a solid ortho-para mixture at 10 K. Due to the rapid conversion of the $J=1$ excited state to the $J=0$ ground state it was not possible to carry out these measurements at constant $J=1$ concentration. Therefore, our measurements represent an average over the changing $J=1$ concentration in the sample. The amount of para-H_2 present in the mixed sample, averaged over the time of the measurements, was estimated to be on the order of 40% using the known conversion rate in the solid;[1] a similar value was obtained by comparing the spectrum with the pure para-H_2 spectrum.

The upper portion of Fig. 7 shows a spectrum of the ortho-para mixture. It is no longer possible to distinguish separate peaks in this spectrum. The scattering function of pure ortho-H_2 can be extracted by subtracting the para-H_2 spectra, multiplied by the concentration, from those of the mixture. The result of this subtraction is shown in the lower portion of Fig. 7. The lines in the spectra of the ortho component still overlap since transitions to all J' states are now possible. It is not possible to assign these lines to individual transitions in any model-independent way. However, using the Young and Koppel calculations for the intensity of the individual transitions we have determined the widths of the peaks in the pure ortho-H_2. These widths are consistent with those determined in the measurements on para-H_2, indicating little dependence of $\langle E_k \rangle$ on the ortho-para ratio.

V. CONCLUSIONS

The principal finding of this experiment is that, within the range of momentum transfer Q studied (5–30 Å^{-1}), the scattering from liquid and solid hydrogen can be described on the basis of transitions between rotational and vibrational states and a Gaussian translational momentum distribution, with little or no coupling between the internal and translational modes.

The mean translational kinetic energy is dominated by the quantum-mechanical zero-point motions for both the solid and the liquid. The kinetic energies are significantly larger than would be predicted on the basis of a simple Debye model and the measured Debye temperatures. Surprisingly, the kinetic energy in the solid is 22% higher than in the liquid, a much larger difference than predicted from the Debye model. Microscopic calculations of the solid by Goldman, which include correlations that are ignored in the Debye model, give better agreement.

The scattering from molecular hydrogen at low Q's (2–5 Å^{-1}) can be interpreted in terms of multiphonon processes.[27] Measurements[3,28,29] at intermediate energy and momentum transfer (50–90 meV) have been attributed to recoil phenomena. However, attempts to interpret the scattering based on an ideal-gas model were not very satisfactory.[3,28] This is not surprising considering the large contribution of the quantum zero-point motion in the solid and liquid. At higher Q's (>5 Å^{-1}) the scattering approaches the limiting form expected for single-particle scattering.

There appear to be real discrepancies between the measured molecular structure factors and those calculated from the Young and Koppel free-rotation model. The origin of these discrepancies is not clear. They may result from coupling of the rotational and vibrational excitations in the molecule. Another possibility is coupling of the rotational moments to the translational motion (crystal-field effects) of the molecule.

ACKNOWLEDGMENTS

We gratefully acknowledge the help of R. Kleb, who constructed the sample cell, and Dr. C. K. Loong during the course of this experiment. We also wish to acknowledge useful conversations with Dr. V. V. Goldman, Dr. K. W. Herwig, and G. J. Kellogg. The project was supported in part by the U.S. Department of Energy, Basic Energy Sciences–Materials Sciences, under Contract Nos. W-31-109-ENG-38 and DE-AC02-76ER01198, by the National Science Foundation under Grant No. DMR-8704288, and by the German Federal Ministry for Research and Technology (BMFT) under Contract No. O3KN1SIE2. One of us (W.L.) wishes to thank the University of Illinois at Urbana-Champaign for financial support.

*Present address: Universität-Gesamthochschule, Siegen, Postfach 101240 D-5900, Siegen, West Germany.

[1]I. F. Silvera, Rev. Mod. Phys. **52**, 393 (1980).

[2]M. Nielsen, Phys. Rev. B **7**, 1626 (1973).

[3]W. Schott, Z. Phys. **231**, 243 (1970).

[4]K. Carneiro, M. Nielsen, and J. P. McTague, Phys. Rev. Lett. **30**, 481 (1973).

[5]R. O. Simmons and P. E. Sokol, J. Phys. C **136b**, 156 (1986).

[6]H. R. Glyde and E. C. Svensson, in *Neutron Scattering,* edited by D. L. Price and K. Sköld (Academic, Orlando, 1987), Pt. B, p. 303.

[7]S. I. Anisimov and Yu. V. Petrov, Zh. Eksp. Teor. Fiz. **74**, 778 (1978) [Sov. Phys.—JETP **47**, 407 (1978)], and references therein.

[8]P. Eisenberger and P. M. Platzman, Phys. Rev. A **2**, 415 (1970).

[9]A. Sjölander, Ark. Fys. **14**, 315 (1958).

[10]V. F. Sears, Can. J. Phys. **63**, 68 (1985).

[11]R. G. Sachs and E. Teller, Phys. Rev. **60**, 18 (1941); J. A. Janik and A. Kowalska, in *Thermal Neutron Scattering,* edited by P. A. Egelstaff (Academic, New York, 1965), p. 413.

[12]A. Griffin and H. Jobic, J. Chem. Phys. **75**, 5940 (1981).

[13]G. Sarma, in *Inelastic Neutron Scattering in Liquids and Soilds* (IAEA, Vienna, 1961), p. 397.

[14]J. U. Young and J. A. Koppel, Phys. Rev. **135A**, 603 (1964).

[15]F. G. Mertens and W. Biem, Z. Phys. **250**, 273 (1972).

[16]V. F. Sears, in *Neutron Scattering,* edtied by K. Sköld and D. L. Price (Academic, Orlando, 1986), Pt. A, p. 521.

[17]B. P. Stoicheff, Can. J. Phys. **35**, 730 (1957).

[18]D. L. Price, J. M. Carpenter, C. A. Pelizzari, S. K. Sinha, I. Bresof, and G. O. Ostrowski, in Proceedings of the Sixth Meeting of the International Collaboration on Advanced Neutron Sources, Argonne National Laboratory, 1982 [Argonne National Laboratory Report No. ANL-82-80, 1983 (unpublished), pp. 207–215].

[19]C. K. Loong and D. L. Price (unpublished).

[20]C. K. Loong, S. Ikeda, and J. M. Carpenter, Nucl. Instrum. Methods A **260**, 381 (1987).

[21]D. L. Price and S. K. Sinha, IPNS Note 51, Argonne National Laboratory, 1982 (unpublished).

[22]P. E. Sokol (unpublished).

[23]R. O. Hilleke, P. Chaddah, R. O. Simmons, D. L. Price, and S. K. Sinha, Phys. Rev. Lett. **52**, 847 (1984).

[24]P. E. Sokol, D. A. Peek, R. O. Simmons, R. O. Hilleke, and D. L. Price, Phys. Rev. B **33**, 7787 (1986).

[25]P. C. Souers, Lawrence Livermore Laboratory Report No. UCRL-52628, 1979 (unpublished).

[26]V. V. Goldman, Phys. Rev. B **20**, 4478 (1979), and private communication.

[27]W. Langel, J. Mol. Struct. **143**, 1 (1986).

[28]W. L. Whittemore and H. R. Danner, in *Inelastic Neutron Scattering in Liquids and Solids* (IAEA, Vienna, 1963), Vol. I, p. 273.

[29]W. Langel, Rev. Phys. Appl. (Paris) **19**, 755 (1984).